

Fatigue Tests on Prestressed Concrete Beams Made With Debonded Strands



Bruce W. Russell
Ph.D., P.E.

Assistant Professor
School of Civil Engineering and
Environmental Science
University of Oklahoma
Norman, Oklahoma



Ned H. Burns, Ph.D., P.E.

Director, Ferguson Structural
Engineering Laboratory
Zarrow Centennial Professor of
Engineering
University of Texas at Austin
Austin, Texas

Six fatigue tests were performed on pretensioned concrete beams containing debonded strands to determine if their behavior would be similar to the behavior observed from statically loaded companion beams. Each initially "precracked" beam specimen was subjected to at least one million cycles of equivalent service load. Periodically, large static overloads were applied to each specimen to simulate the relatively large permit loads that some structures may be required to resist, and to increase strand bonding requirements. Loads, deflections, and strand slips were measured at significant intervals and beam behaviors were observed. After completion of fatigue testing, the beams were loaded statically until failure. The tests demonstrated that although repeated loading may cause some additional slippage, the strand slips remained quite small and did not affect the overall beam behavior. Furthermore, the ultimate behavior of these beams verifies that the prediction for bond failure is dependent on the propagation of cracking through the transfer zone of a debonded strand, confirming similar results obtained from static tests.

The debonding, or blanketing, of strands is an alternative method to draping strands for controlling the maximum tensile and compressive stresses in the end regions of pretensioned concrete beams. Debonding strands can simplify girder construction by allowing straight strand patterns and eliminating draped strands. Draping strands is more difficult and poses greater hazards to worker safety. Therefore, debonding

strands may present the producer with an economical alternative to draping strands.

This paper presents the results of six fatigue tests performed on pretensioned concrete beams that contained debonded strands. These test results are presented here as the second paper in a series of three papers dealing with the structural behavior of prestressed concrete beams made with debonded strands. The first paper¹ presented the

theoretical background predicting the behavior associated with pretensioned beams made with debonded strands, plus the results from static testing. The third and final paper will contain specific design recommendations for the safe and reliable use of debonded strands in prestressed concrete beams.

The fatigue test specimens are companion specimens to a series of beams that were tested statically (monotonically) to establish the anchorage behavior of debonded strands.^{1,2,3} In the static tests, strand slip and general anchorage failure occurred as a direct result of cracking (either shear cracking or flexural cracking) that propagated through the transfer zones of pretensioned strands.

Furthermore, anchorage failures were prevented in beams where the beam design effectively prevented cracking in the debond/transfer zone (the region of the beam, near the ends, that includes the debonded length plus the transfer zone of debonded strands). From these results, it was concluded that beams can be safely designed using debonded strands if the debonding pattern is designed so that the transfer zone of the debonded strands does not extend into regions of the beam where cracking is produced from ultimate loading.

From the static test series, small amounts of strand slip were observed, indicating the possibility that additional load cycles would further deteriorate strand anchorage. Fatigue tests were performed to determine:

1. How much additional bond deterioration would result under fatigue loading.
2. If beams tested in fatigue behaved similarly to their statically tested companions.
3. If the correlation between cracking and anchorage failure remains consistent.

Altogether, six fatigue tests were performed on four beam specimens. Each test subjected the beam to a minimum of one million cycles of fatigue, unless premature failure occurred from fatigue or an intermediate static loading. Static load tests were performed at initial loading and at intermediate stages to test the beams for loss of stiffness or loss of bond. These

intermediate static loads were overloads that exceeded the service load by factors of 1.3 to 1.6 to simulate large truck traffic or special permit loads that a bridge must sometimes support in the course of its service life. Each beam was "precracked" prior to fatigue testing.

In general, the behavior of the beam specimens subjected to fatigue matched the behavior of the statically tested beams. In the fatigue specimens, anchorage failures were caused by cracking that propagated through or near the transfer zone of debonded strands (the debond/transfer zone), just as in the beams that were tested statically. Furthermore, strand slips showed a significant tendency to stabilize under repeated loading; additional bond slips occurred largely through the application of large static overloads and not as a result of repeated applications of service load. Most importantly, these fatigue tests demonstrated that the anchorage of debonded strands can be ensured by designing the debonded length so that cracking is not likely to intersect the transfer zone of the debonded strand.

CURRENT AASHTO AND ACI CODE REQUIREMENTS

Current code provisions of the American Concrete Institute (ACI)⁴ and the American Association of State Highway and Transportation Officials (AASHTO)⁵ governing the use of debonded strands require doubling the basic development length from that of fully bonded strand. An exception is allowed when the beams are designed so that the bottom fiber of the beam will remain in compression under service load.

The two times provision is based largely on empirical data obtained from tests conducted by Kaar and Magura.⁶ In these tests, beam failures were caused by anchorage failure of debonded strands when the bonded length was only one times the bonded length given by Section 12.9.1 of the ACI Building Code.⁴ On the other hand, when twice the bonded length was provided, the strands were fully developed and the beams failed in flexure.

In 1979, tests conducted by Rabbat Kaar, Russell, and Bruce^{7,8} demonstrated that when zero tension was allowed in the concrete at service load, debonded strands required only one times the development length given by ACI 12.9.1.

Current code provisions reflect the behavioral uncertainty that surrounds debonded strands. Even though the AASHTO Specifications allow debonded strands, many state Departments of Transportation (DOTs) do not allow their use because of concerns that debonding strands may adversely affect the performance of pretensioned beams. For example, the Texas DOT currently does not allow debonded strands as an alternative to draping for I-shaped girders, but does employ debonded strands in box shapes and other cross sections.

THEORETICAL DEVELOPMENT

In early research conducted on anchorage of pretensioned wires, Janney (1954)⁹ predicted that strand anchorage failures resulted from a "wave of high bond stress" that reaches the transfer zones of pretensioned wires. He reasoned that because prestress bond developed largely through the wedging action from Hoyer's effect, bond failure would result if the strand in the transfer zone was required to carry additional tension. Increases in strand tension cause the strand diameter to diminish; consequently, wedging action is destroyed. Flexural tests conducted by Hanson and Kaar¹⁰ verified that pretensioned anchorage was destroyed when strand tension increased near the transfer zone.

Research at the University of Texas at Austin^{1,2,3,11,12} demonstrated that increases in strand tension and subsequent anchorage failure are caused by cracking that propagates through or near the transfer zone of a pretensioned strand. When a crack forms in concrete, tension in the prestressing steel must increase to resist widening of the concrete crack. The additional tension in the strand is resisted by bond stresses between the concrete and steel. (Note that poor bond quality is evidenced by wide spacing between

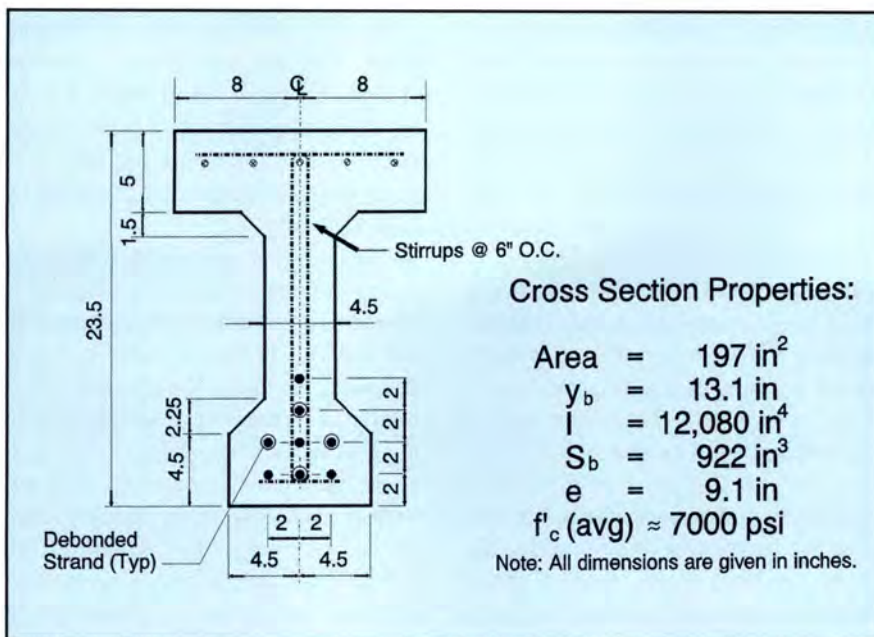


Fig. 1. Cross section details.

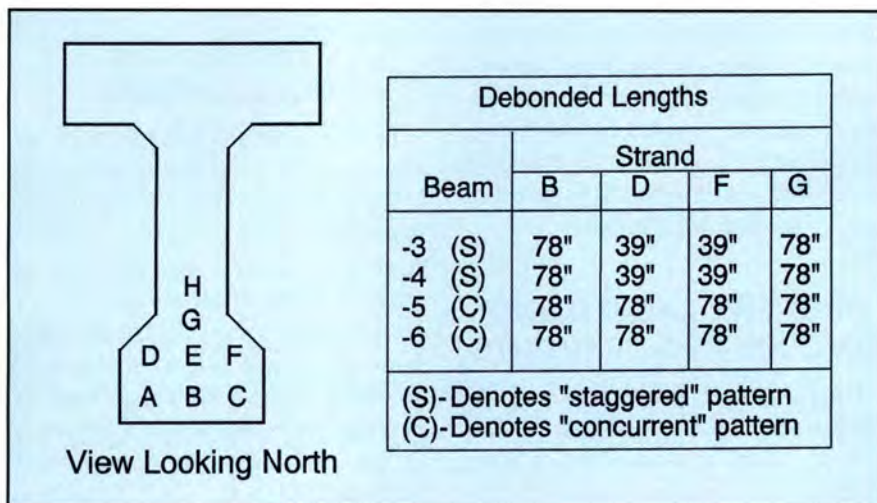


Fig. 2. Strand pattern and debonding schedule.

Table 1. Variables by test specimen for repeated load tests.

| Test | Beam length, L (in.) | Debonded length, L_b (in.) | Embedment length, L_e (in.) | Type of debonding* |
|-----------|------------------------|------------------------------|-------------------------------|--------------------|
| DB850-F1A | 480 | 78 | 100 | S |
| DB850-F1B | 480 | 78 | 80 | S |
| DB850-F2A | 480 | 78 | 80 | S |
| DB850-F2B | 480 | 78 | 110 | S |
| DB850-F3 | 480 | 78 | 120 | C |
| DB850-F4 | 480 | 78 | 100 | C |

Note: 1 in. = 0.0254 m.

* "S" denotes staggered debonding; "C" denotes concurrent debonding.

flexural cracks as well as large crack widths.) Local bond slip of the strand must occur over some finite distance immediately adjacent to the crack, and roughly corresponds to increased tension in the strand. In this manner,

cracking near the transfer zone causes the "wave of high bond stress" that leads to anchorage failure.

A behavioral model for predicting the bond failure of debonded prestressing strands was presented in the

first publication of this series.¹ The prediction for bond failure is directly related to a prediction for cracking through or near the transfer zone of a prestressing strand. In beams with debonded strands, anchorage failure of the debonded strands is caused by cracking through the transfer zones of the debonded strands, the debond/transfer zone. Furthermore, because cracking in the concrete can be reliably predicted, bond failure of the prestressing strand can also be predicted.

TEST PROGRAM

Specimen Description

Each of four I-shaped specimens was cast monolithically. A detailed cross section of the beams is shown in Fig. 1. Section properties are also given in the figure. Each beam contained vertical shear reinforcement; pairs of No. 3 bar stirrups were spaced at 6 in. (152 mm) on center without variance along the length of each beam. No special confining steel or anchorage details were provided on any strand.

Each beam was 40 ft (12.2 m) in length with eight 0.5 in. (12.7 mm) diameter strands in each beam, four of which were debonded. The debonding schedule is shown in Fig. 2. The strands are labeled by letters of the alphabet, A through G, to simplify the reporting of observations.

The debonding schedule notes that Beams DB850-F1 and DB850-F2 contain debonding patterns labeled "staggered," denoting a debonding pattern where debonded length varies from strand to strand. For Beams DB850-F1 and DB850-F2, the debonded length for Strands B and G is 78 in. (1.98 m) whereas the debonded length for Strands D and F is only 39 in. (0.99 m). Conversely, the debonding pattern in Beams DB850-F3 and DB850-F4 is labeled "concurrent," meaning that the debonded length is the same for all debonded strands, 78 in. (1.98 m).

The debonded lengths were selected to test strand embedment lengths between 1.0 and 2.0 times the basic development length given in ACI 12.9⁴ and AASHTO Eq. (9-32)⁵ (reasons for choosing a debonded length depend on the cross section tested and are ex-

plained in greater detail in Ref. 1). Beams with concurrent debonding were included in the test series to highlight special behaviors associated with debonded strands; concurrent debonding is not recommended in practice.

Variables

The variables tested on the debonded beams included:

1. Type of debonding cutoff [staggered (S) or concurrent (C)]
2. Embedment length, L_e
3. Number of load cycles, N
4. Magnitude and frequency of intermediate static overloads

Table 1 gives the debonded length, the type of debonding, and the embedment length for each test specimen. The length of debonding is measured from the end of the beam to the furthest extent of debonding; if a debonding pattern is staggered, the reported debonded length is that of the longest debonded length.

Embedment length is defined as the distance from the debond termination point to the load point. Fig. 3 illustrates that the embedment length, L_e , for Beam DB850-F1, Test B was 80 in. (2.03 m). The variables, including the embedment length, the number of load cycles, and the magnitude of the intermediate static overloads were varied for each test, based on results from previous testing. These variations are described in greater detail in the body of the paper.

Fabrication of Test Specimens

Each beam was constructed using the following procedure:

1. Stress strands to 75 percent f_{pu} [202.5 ksi (1400 MPa)]
2. Place the mild steel reinforcement
3. Install the debonding material
4. Construct the formwork
5. Cast the concrete
6. Cure the concrete in place (approximately 2 days)
7. Release the pretensioning (approximately 48 hours after casting)

The debonding material consisted of split plastic tubing, made from semi-rigid plastic. It was installed on the strands where debonding was required; its natural curl wrapped it to

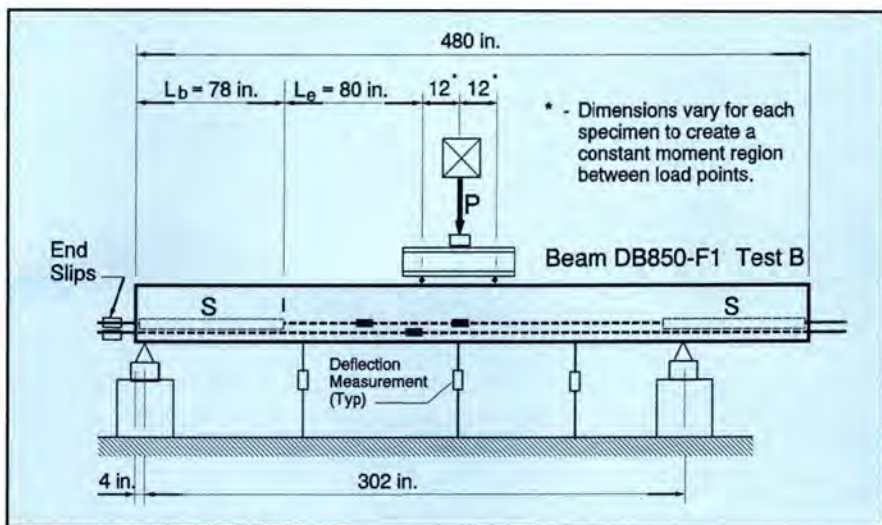


Fig. 3. Typical test setup for beams with debonded strands.

the strand and provided a reasonably tight fit. Debonding was sealed by taping each end of the debonding tube, but the seam at the longitudinal split fit tightly and was not taped.

The age of the specimens at testing varied due to the length of time required to perform fatigue testing. Significantly, the age of these beams is greater than the age of the companion beams that were tested statically.¹³ For instance, Beam DB850-F1, the first beam tested in the fatigue series, was tested at an age of about 261 days; Beam DB850-F4, the last beam tested in the series, was tested at an average age of 367 days. This contrasts to the statically tested companion specimens that were, on average, only 60 days old at time of testing.

Materials

Prestressing strand was donated by Florida Wire and Cable Company (FWCC). The strand surface was "mill condition" as furnished, having been free from exposure to weathering environments. The strand was maintained in its original condition, as much as possible, throughout the fabrication period. The strand's ultimate strength was specified at 270 ksi (1860 MPa). The seven-wire, low relaxation prestressing strand used for these tests is the current industry standard. The strand's ultimate strength was 283 ksi (1950 MPa), as reported by the manufacturer.

Concrete strengths were designed to

Table 2. Concrete strengths for repeated load tests.

| Beam | Release strength (psi) | Strength at flexural test (psi) | |
|---------|------------------------|---------------------------------|------------|
| | | Moist cure | Field cure |
| DB850-1 | 4642 | 7408 | 7004 |
| DB850-2 | 4043 | 8349 | — |
| DB850-3 | 4396 | 7020 | 7488 |
| DB850-4 | 4805 | — | 7339 |

Note: 1 psi = 0.006895 MPa.

be 4500 psi (31 MPa) at release and 6000 psi (41 MPa) for 28-day strength. Concrete strengths for the DB850 series beams are listed in Table 2.

Testing Apparatus

A typical test setup is shown in Fig. 3; the dimensions illustrate the setup and test geometry for Beam DB850-F1, Test B. As shown, the embedment length, L_e , for this test was set at 80 in. (2.03 m) and the debonded length was 78 in. (1.98 m). The "S" over the debonded portion of the beam depicts "staggered debonding."

The embedment length, L_e , and span were varied for each test. A constant moment region 24 in. (610 mm) long was assured for each test by choosing the appropriate geometry. Fig. 4 shows Beam DB850-F1 in position to be tested.

A load controlled, closed loop system applied force to each specimen during the fatigue loadings. The final static test and intermediate static tests were performed with a static hydraulic system to ensure safety.

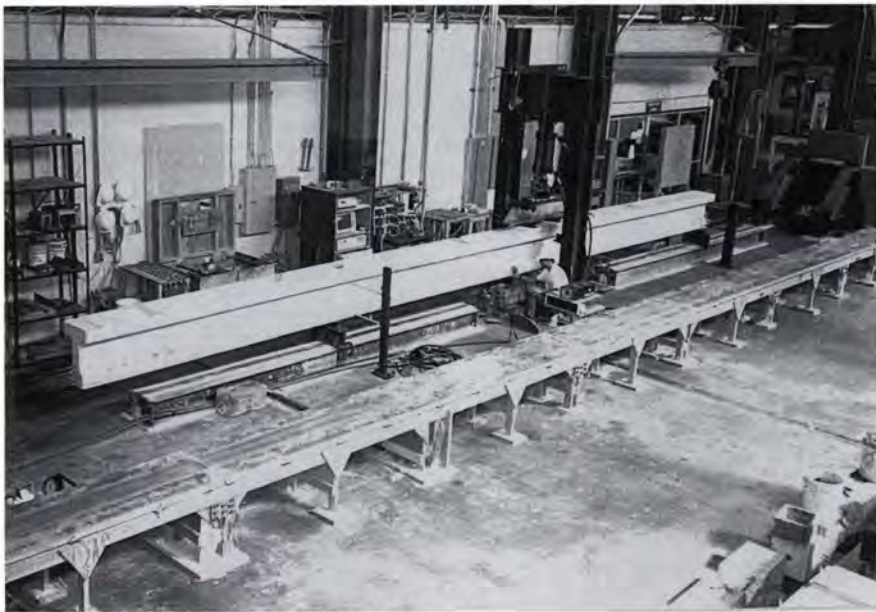


Fig. 4. Test setup showing Beam DB850-F1.



Fig. 5. Electronic potentiometers to measure end slip.

Instrumentation

Instrumentation measured the applied load, beam deflections, strand end slips, and strand strains at specified locations. These data were measured electronically and stored by the data acquisition system. Load was measured from an electronic load cell at the point of load application. Deflection and end slips were measured by linear potentiometers. All of the electronic instruments were calibrated prior to testing. Top fiber concrete strains were measured in the constant moment region for each test using mechanical strain gauges.

End slips were measured on seven of the eight strands. The four debonded strands, Strands B, D, F and G, were monitored for end slip on each test. Strand E was the only strand not monitored for end slip due to geometric constraints at the ends of the beams. (Strand E was fully bonded for all tests and no visible signs of end slips occurred.) Fig. 5 shows the linear potentiometers that were used to measure end slips electronically. End slip measurements of 0.001 in. (0.025 mm) were detected, thus, even very small strand slips did not escape notice.

Fatigue Loads, Static Loads, and Stress Ranges

Each test began with an initial static flexural test to “precrack” the beam, followed by fatigue loading for at least one million cycles. Each load cycle

varied load from a minimum of 25 percent to a maximum of 100 percent of the equivalent design service load, P_{sv} . The equivalent design service load, P_{sv} , is defined as the load required to cause a bottom fiber tension equal to $6\sqrt{f'_c}$, as calculated for the uncracked section.

The purpose of the initial static loading was to “precrack” each specimen so that the stress range of the prestressing steel would be larger than the stress range required for an uncracked beam. Previous fatigue tests had shown that little distress occurs before flexural cracks develop.^{8,13,14,15} More

importantly, as the stress range of the prestressing steel increases, the bond stresses between steel and concrete must also increase. Therefore, a higher stress range places greater demand on related bond stresses.

The strand stress range for these tests is illustrated in Fig. 6, where applied moment is plotted vs. strand stress. Strand stresses were computed using the compatible strains method, assuming pure flexural behavior for both cracked and uncracked beam sections. The effective prestress, f_{se} , was computed to be approximately 152 ksi (1050 MPa) based on elongation mea-

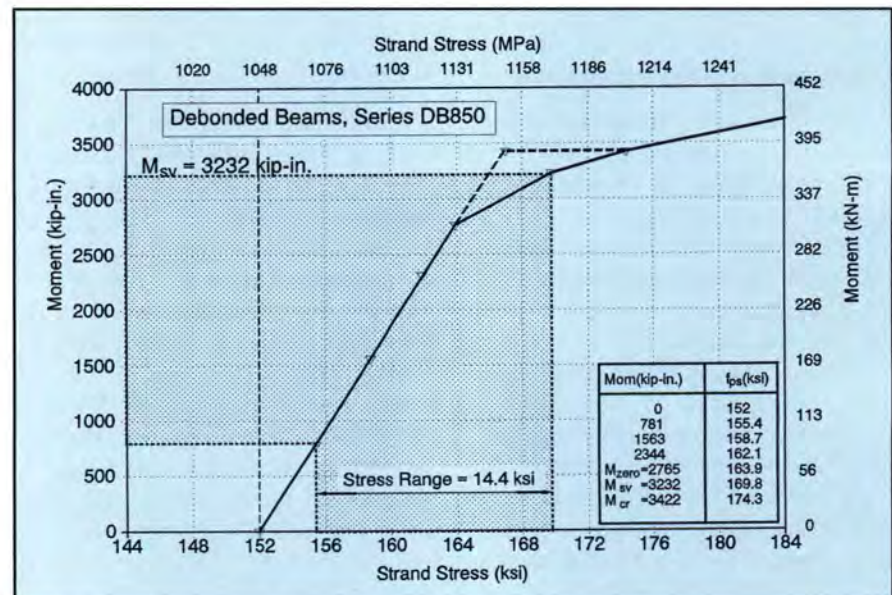


Fig. 6. Stress range for fatigue tests.

Table 3. Summary of beam deflections and strand slips from static tests on Beam DB850-F1, Test A.

| Load cycle <i>N</i> | Maximum load (kips) | Percent P_{sv} | Deflections | | | Slip B | | Slip G | |
|------------------------|------------------------|---------------------|-------------|-------|-------------|-----------|--------|-----------|--------|
| | | | Beginning | End | at P_{sv} | Beginning | End | Beginning | End |
| 1 | 62.3 | 1.6 | 0 | 0.129 | 0.63 | 0 | 0.0209 | 0 | 0.0217 |
| 1023 | 62.4 | 1.6 | 0.127 | 0.154 | 0.97 | 0.0296 | 0.0867 | 0.035 | 0.0522 |
| 134,912 | 62.4 | 1.6 | 0.197 | 0.215 | 1.08 | 0.087 | 0.128 | 0.052 | 0.071 |
| 381,864 | 50.0 | 1.3 | 0.23 | 0.24 | 1.14 | 0.128 | 0.128 | 0.072 | 0.071 |
| 524,053 | 50.0 | 1.3 | 0.29 | 0.29 | 1.18 | 0.128 | 0.128 | 0.071 | 0.071 |
| 703,174 | 50.0 | 1.3 | 0.29 | 0.29 | 1.17 | 0.128 | 0.128 | 0.072 | 0.072 |
| 1,040,050 | 70.1 | 1.8 | 0.29 | 0.35 | 1.17 | 0.128 | 0.240 | 0.072 | 0.176 |

Note: 1 in. = 0.0254 m; 1 kip = 4.448 kN.

$L_c = 100$ in.; $P_{sv} = 40.4$ kips; $P_u = 75.1$ kips.

Table 4. Summary of beam deflections and strand slips from static tests on Beam DB850-F1, Test B.

| Load cycle <i>N</i> | Maximum load (kips) | Percent P_{sv} | Deflections | | | Slip B | | Slip G | |
|------------------------|------------------------|---------------------|-------------|-------|-------------|-----------|--------|-----------|--------|
| | | | Beginning | End | at P_{sv} | Beginning | End | Beginning | End |
| 1 | 58.5 | 1.25 | 0 | 0.06 | 0.56 | 0 | 0.0002 | 0 | 0.0003 |
| 432 | 58.9 | 1.3 | 0.029 | 0.039 | 0.73 | 0.0005 | 0.0006 | 0.0008 | 0.0004 |
| 54,534 | 58.9 | 1.3 | 0.075 | 0.081 | 0.70 | 0.0009 | 0.0009 | 0.0003 | 0.0002 |
| 158,000 | 58.9 | 1.3 | 0.094 | 0.094 | 0.73 | 0.0011 | 0.0017 | 0.0002 | 0.0008 |
| 386,878 | 72.5 | 1.6 | 0.094 | 0.159 | 0.74 | 0.0010 | 0.1292 | 0.0004 | 0.0862 |
| 1,027,083 | 82.6 | 1.75 | 0.188 | 0.311 | 0.77 | 0.159 | 0.605 | 0.093 | 0.5520 |

Note: 1 in. = 0.0254 m; 1 kip = 4.448 kN.

$L_c = 80$ in.; $P_{sv} = 47.1$ kips; $P_u = 95.0$ kips.

measurements at stressing, strand strain gauge data, and approximated losses using the method outlined by Zia et al.¹⁶ and adopted by PCI.¹⁷

Strand stresses are computed from the strain at the centroid of the prestressing steel, and using the stress vs. strain relationship supplied by the manufacturer of the strands. The figure indicates that the stress range was 14.4 ksi (99 MPa) for the beams tested. For an uncracked beam, the stress range would be approximately 10 ksi (69 MPa).

Periodically, fatigue testing was interrupted to conduct a static flexural test. During these intermediate tests, overloads (loads greater than service load) were statically applied to simulate heavier than usual truck traffic or permit loads that regularly occur within the life of a bridge. Overman et al.¹³ noted that occasional modest overloads can produce extremely detrimental effects on the fatigue behavior of prestressed concrete beams.

In general, overloads varied from 1.3 times the service load to 1.6 times the service load. After an overload cycle, fatigue loading was continued as before, with repeated loads varying between 25 and 100 percent of service

load. Intermediate static overloads frequently caused additional damage to the beam in the form of additional end slips or additional cracking. After completion of at least one million cycles, each beam was then loaded statically until failure. Two beams, Beams DB850-F2B and DB850-F4, failed during intermediate load tests and were not loaded for one million fatigue cycles.

For each static test (including initial static tests, intermediate static overloads, and the final static test to failure), the load was increased at regular increments by increasing the hydraulic pressure supplied to the actuator. Data and measurements were recorded at every load increment, approximately 2.0 to 5.0 kip (9 to 22 kN) increments, until cracking. Cracking loads and crack locations were noted and recorded.

All special or unique behaviors were noted and crack patterns were marked with a broad ink marker on the specimen. End slips were noted and recorded. Failure was defined by the beam's inability to sustain load through increasing deformations. Flexural failures resulted when the top flange of the beam failed in compression.

Anchorage failures resulted in general slip of the strand relative to the concrete and a sudden loss of capacity.

Beams DB850-F1 and DB850-F2 were each tested twice, once at each end. The first test on each specimen is designated "Test A" while the second test is designated "Test B." Two tests were possible on these beams because the first test (Test A) did not damage the anchorage zone at the opposite end of the beams. In the cases of Beams DB850-F3 and DB850-F4, longer development length requirements (because of "concurrent" debonding) precluded an effective second test.

TEST RESULTS

In reviewing the test results, the mode of failure, either flexural failure or bond failure, is the primary indicator of anchorage performance. Flexural failures are evidenced by crushing of the concrete after yielding of the strand. Furthermore, flexural failures are characterized by the capability of a beam to resist the nominal flexural moment, combined with the ability to sustain load through large deformations. By meeting the dual criteria of capacity and ductility, a beam demon-

Table 5. Summary of beam deflections and strand slips from static tests on Beam DB850-F2, Test A.

| Load cycle <i>N</i> | Maximum load (kips) | Percent P_{sv} | Deflections | | | Slip B | | Slip G | |
|------------------------|------------------------|---------------------|-------------|-------|-------------|-----------|-------|-----------|-------|
| | | | Beginning | End | at P_{sv} | Beginning | End | Beginning | End |
| 1 | 55.0 | 1.3 | 0 | 0.086 | 0.61 | 0 | 0.087 | 0 | 0.081 |
| 7000 | 42.5 | 1.05 | 0.091 | 0.096 | 1.06 | 0.292 | 0.293 | 0.355 | 0.356 |
| 26,310 | 42.5 | 1.05 | 0.116 | 0.122 | 1.12 | 0.325 | 0.326 | 0.396 | 0.395 |
| 121,308 | 55.0 | 1.3 | 0.141 | 0.159 | 1.20 | 0.327 | 0.358 | 0.396 | 0.417 |
| 192,945 | 63.8 | 1.5 | 0 | 0.543 | 1.18 | 0.383 | 0.602 | 0.472 | 0.676 |

Note: 1 in. = 0.0254 m; 1 kip = 4.448 kN.

$L_e = 80$ in.; $P_{sv} = 41.97$ kips; $P_u = 78.1$ kips.

Table 6. Summary of beam deflections and strand slips from static tests on Beam DB850-F2, Test B.

| Load cycle <i>N</i> | Maximum load (kips) | Percent P_{sv} | Deflections | | | Slip B | | Slip G | |
|------------------------|------------------------|---------------------|-------------|-------|-------------|-----------|------|-----------|-------|
| | | | Beginning | End | at P_{sv} | Beginning | End | Beginning | End |
| 1 | 61.6 | 1.3 | 0 | 0.086 | 0.60 | 0 | 0 | 0 | 0 |
| 87,000 | 47.0 | 1.0 | 0.114 | – | 0.78 | 0 | 0 | 0 | 0 |
| 184,410 | 65.0 | 1.4 | 0.141 | 0.164 | 0.80 | 0 | 0 | 0 | 0 |
| 271,194 | 60.0 | 1.3 | 0.175 | 0.181 | 0.91 | 0 | 0 | 0 | 0 |
| 1,110,222 | 81.4 | 1.8 | 0.175 | – | 0.97 | 0 | 0.20 | 0 | 0.125 |

Note: 1 in. = 0.0254 m; 1 kip = 4.448 kN.

$L_e = 110$ in.; $P_{sv} = 46.95$ kips; $P_u = 87.3$ kips.

Table 7. Summary of beam deflections and strand slips from static tests on Beam DB850-F3.

| Load cycle <i>N</i> | Maximum load (kips) | Percent P_{sv} | Deflections | | | Slip B | | Slip G | |
|------------------------|------------------------|---------------------|-------------|-------|-------------|-----------|--------|-----------|--------|
| | | | Beginning | End | at P_{sv} | Beginning | End | Beginning | End |
| 1 | 57.7 | 1.3 | 0 | 0.086 | 0.60 | 0 | 0.0018 | 0 | 0 |
| 62,418 | 58.0 | 1.3 | – | – | – | 0.0016 | 0.0025 | 0 | 0.0002 |
| 152,538 | 65.0 | 1.5 | 0.174 | 0.203 | 0.847 | 0.0017 | 0.0022 | 0.0002 | 0.0002 |
| 414,844 | 55.0 | 1.3 | 0.203 | 0.215 | 0.920 | 0.0031 | 0.0033 | 0.0455 | 0.0475 |
| 1,085,569 | 74.2 | 1.7 | 0.234 | 0.481 | 0.947 | 0.0025 | 0.459 | 0.0479 | 0.418 |

Note: 1 in. = 0.0254 m; 1 kip = 4.448 kN.

$L_e = 120$ in.; $P_{sv} = 43.59$ kips; $P_u = 81.1$ kips.

Table 8. Summary of beam deflections and strand slips from static tests on Beam DB850-F4.

| Load cycle <i>N</i> | Maximum load (kips) | Percent P_{sv} | Deflections | | | Slip B | | Slip G | |
|------------------------|------------------------|---------------------|-------------|------|-------------|-----------|-------|-----------|-------|
| | | | Beginning | End | at P_{sv} | Beginning | End | Beginning | End |
| 1 | 55.9 | 1.2 | 0 | 0.05 | 0.54 | 0 | 0 | 0 | 0 |
| 135,652 | 55.0 | 1.2 | – | – | 0.71 | 0.003 | 0.003 | 0.003 | 0 |
| 266,147 | 69.3 | 1.5 | – | – | – | 0.0025 | 0.336 | 0 | 0.323 |

Note: 1 in. = 0.0254 m; 1 kip = 4.448 kN.

$L_e = 100$ in.; $P_{sv} = 46.12$ kips; $P_u = 85.8$ kips.

strates that its load capacity is predictable and that reasonable warning occurs before collapse, thereby providing a safe and reliable structure. Flexural failures also suggest that the strand anchorage is sufficient to develop the tension required to resist the ultimate flexural moment.

Anchorage failures, also called bond failures, are characterized by general slip of one or more strands through the concrete, as measured by end slips. Typical anchorage failures are unable to develop the nominal flexural capac-

ity of the beam. It is interesting to note that anchorage failures on beams with debonded strands can be ductile failures because the anchorage of fully bonded strands is capable of developing enough strand tension to ensure strand yielding. This is an important observation that may allow a greater margin of safety for anchorage failure of debonded strands than for anchorage failures in fully bonded beams where bond failures may result in sudden and explosive collapse.^{2,12}

In the next six subsections, the re-

sults from each test are discussed briefly. Loading histories for each test are described in both tabular and graphical form. Tables 3 through 8 list the magnitude and frequency of each intermediate static overload. These tables also list the values for strand slips and beam deflections. Increasing strand slips indicate deterioration of strand anchorage. Similarly, increasing deflections indicate a deterioration of beam stiffness.

The load histories and end slips are plotted graphically in the companion

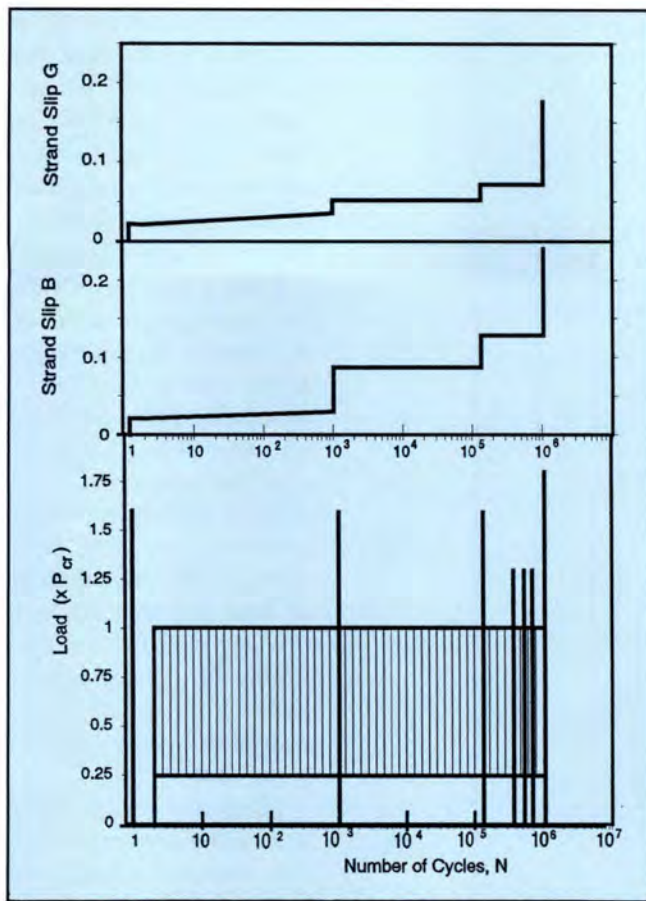


Fig. 7. Strand slips vs. number of load cycles and loading history for Beam DB850-F1, Test A.

figures, plotting load cycles on log scale vs. the magnitude of each load cycle and the measured strand slips on Strands B and G. Results of the final static tests are described graphically where loads and end slips are plotted vs. beam deflection. Also included in these figures are the loading geometry for each test.

Beam DB850-F1, Test A

With an embedment length of 100 in. (2.54 m), this test can be compared with a companion beam from the static test series, Beam DB850-4B, reported in Ref. 1. Both beams possessed identical cross sections, debonding patterns and embedment lengths. The statically tested beam, Beam DB850-4B, failed in flexure; strand anchorage was wholly sufficient to develop the strand tension required to produce the nominal flexural capacity.

As shown in Table 3, the initial static test loaded the beam to a maximum flexural load of 62.3 kips (277 kN), or 1.6 times the service load, P_{sv} . At this load, a flexural crack formed at Station 105 [105 in. (2.67 m) from the end of the beam], very near the theoretical transfer zone of the debonded strands {the theoretical debond/transfer zone extends to 103 in. (2.6 m) [78 in. (1.98 m) debonded length plus 25 in. (635 mm) transfer length¹⁸] from the end of the beam}. Upon formation of the crack at Station 105, strand slips were initiated on both Strands B and G; each measured about 0.02 in. (0.05 mm).

Fatigue loading commenced after completion of the initial static test. The loading history and strand slips are plotted in Fig. 7. These data are also summarized in Table 3. Load was varied between a maximum load equal to the service load, P_{sv} , and a minimum load approximately equal to 25 percent of P_{sv} . End slips increased slightly through the early repeated load cycles, from 0.02 in. (0.05 mm) to about 0.03 in. (0.08 mm) through the first 1000 cycles.

At load cycle 1023, a second static overload test to $1.6 P_{sv}$ was conducted and end slips increased from 0.03 to 0.09 in. (0.08 to 2.3 mm) for Strand B and to approximately 0.05 in. (1.3 mm)

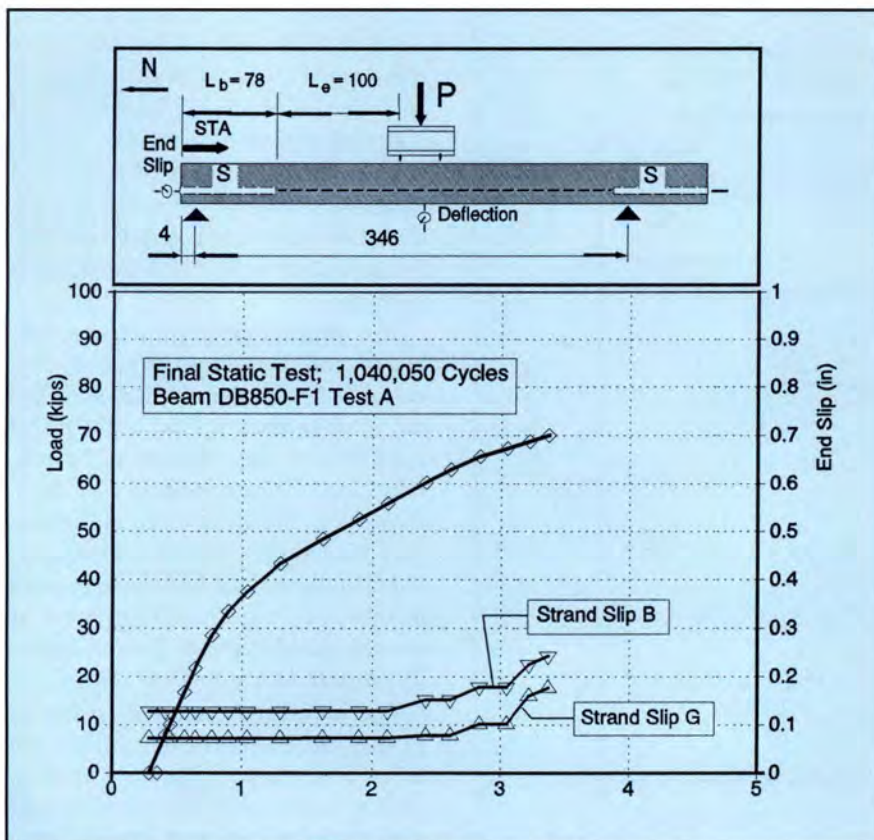


Fig. 8. Load vs. deflection and end slips for Beam DB850-F1, Test A.

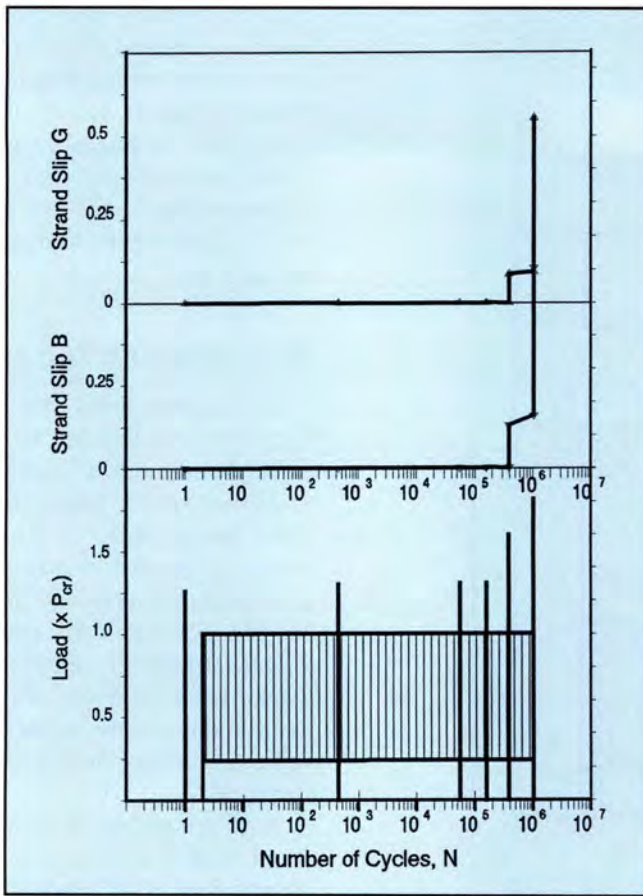


Fig. 9. Strand slips vs. number of load cycles and loading history for Beam DB850-F1, Test B.

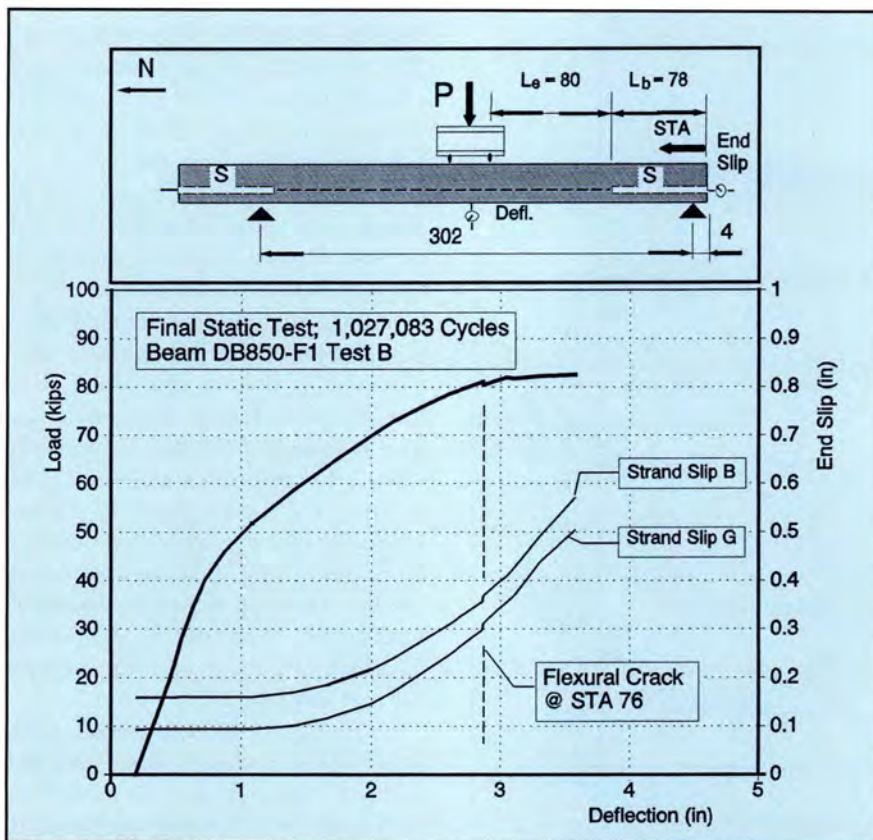


Fig. 10. Load vs. deflection and end slips for Beam DB850-F1, Test B.

for Strand G. Additional repeated loads caused no increases in strand slip. At load cycle 134,912, a third static overload equal to $1.6 P_{sv}$ was applied to the beam. Again, strand slips increased in response to the overload and again, additional repeated loads failed to produce any additional strand slips.

Table 3 also records the beam deflections throughout the beam's loading history. Deflection was measured at the load point. "Zero" deflection equaled the beam deflection before application of any loads. The "Beginning" deflection refers to the absolute deflection before application of a specific load cycle. The "End" deflection refers to the absolute deflection after all loads had been removed at completion of a specific load cycle. The deflection "at P_{sv} " shows the absolute deflection during the test when the equivalent service load, P_{sv} is applied to the beam.

The deflection data indicate that the beam did not undergo any loss in stiffness through the application of 1 million load cycles. Note that in the initial static test, the deflection at service load is significantly less than for other load cycles because the beam has not yet been cracked.

After 1,040,000 cycles, the beam was loaded statically until it failed at an applied load of 70.1 kips (312 kN) with end slips of 0.24 in. (6.1 mm) on Strand B and 0.18 in. (4.6 mm) on Strand G. Load vs. deflection is illustrated in Fig. 8. Measured end slips for Strands B and G are also shown in the figure.

The applied ultimate moment at failure of 5602 kip-in. (633 kN-m) was calculated from the ultimate load and the load geometry. The beam failed from flexure with crushing of the concrete in the top compression fibers. However, the failure moment was only 93 percent of the ultimate capacity of its statically tested companion beam, and only about 93 percent of the calculated nominal flexural capacity, $M_n = 6010$ kip-in. (679 kN-m).

The measured concrete strains at failure may explain why the beam failed at a reduced flexural capacity. Strains measured at the top fiber indicate that the concrete crushed at a strain of about 0.0025 in./in., some-

what lower than expected for crushing strain. A concrete crushing strain smaller than 0.003 was noted in several of the fatigue tests, indicating creep fatigue or creep rupture (load duration effects) possibly contributed to reducing concrete strength.

Beam DB850-F1, Test B

For this test, an embedment length equal to 80 in. (2.03 m) was chosen. A statically tested companion beam, Beam DB850-3A reported in Ref. 1, also with an embedment length of 80 in. (2.03 m) and staggered debond length of 78 in. (1.98 m), failed in bond (anchorage failure). The relatively short embedment length was selected to determine if anchorage failure could be caused by the application of repeated service loads. The initial static load and subsequent intermediate loads were limited to $1.3 P_{sv}$ to prevent extensive cracking. The loading history and end slips are shown in Fig. 9. Values for end slips and beam deflections are listed in Table 4.

At the initial static load, flexural cracking extended to Station 130 [130 in. (3.30 m) from the end of the beam] and did not affect the anchorage of the strands significantly. Accordingly, there was no appreciable strand slip caused by the initial static load. Also, additional strand slips that occurred during the early repeated loads remained very small.

After 386,878 load cycles, the beam was loaded to $1.6 P_{sv}$. At this loading, flexural cracking propagated through the transfer zone of the debonded strands at Station 88, well within the debond/transfer zone. Upon formation of this crack, strand slips were initiated and measured to be about 0.13 in. (3.3 mm) on Strand B and 0.086 in. (2.2 mm) on Strand G. Application of additional repeated loading caused only slight increases in strand slip.

The final static test was performed after 1,027,083 cycles. Load vs. deflection and end slips are illustrated in Fig. 10. Note that after the decompression load was reached [around 45 kips (200 kN) and indicated by the beam's change in stiffness], increases in strand slip corresponded with increased loading until failure. The

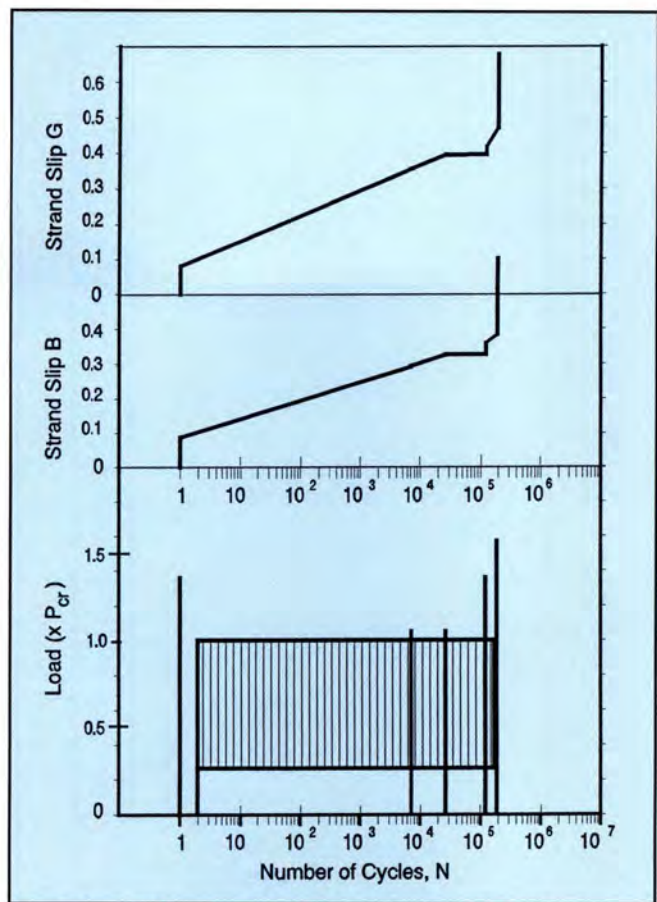


Fig. 11. Strand slips vs. number of load cycles and loading history for Beam DB850-F2, Test A.

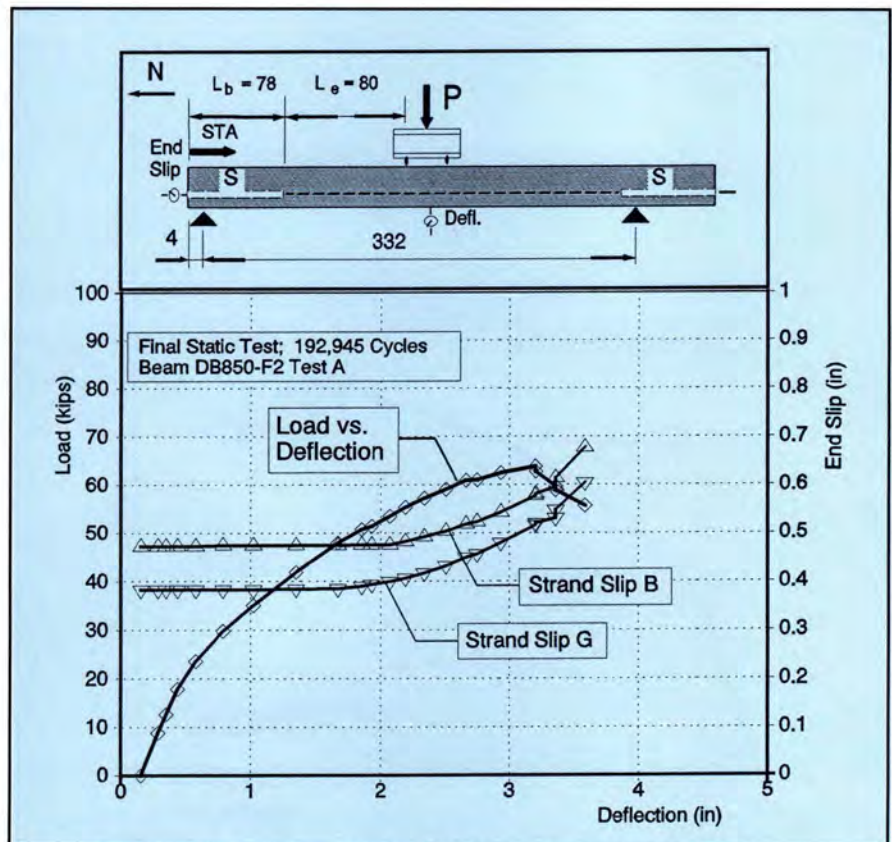


Fig. 12. Load vs. deflection and end slips for Beam DB850-F2, Test A.

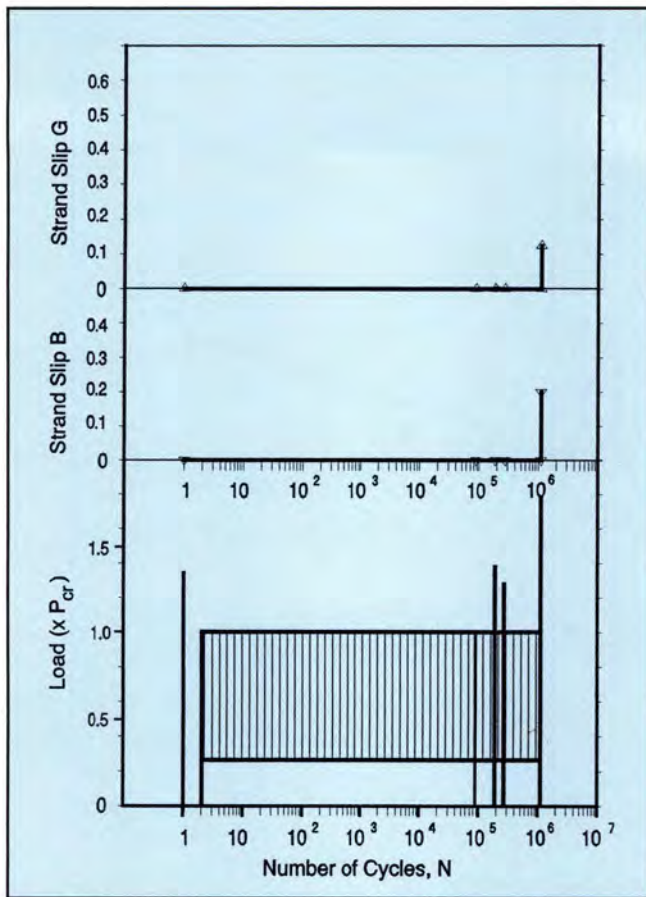


Fig. 13. Strand slips vs. number of load cycles and loading history for Beam DB850-F2, Test B.

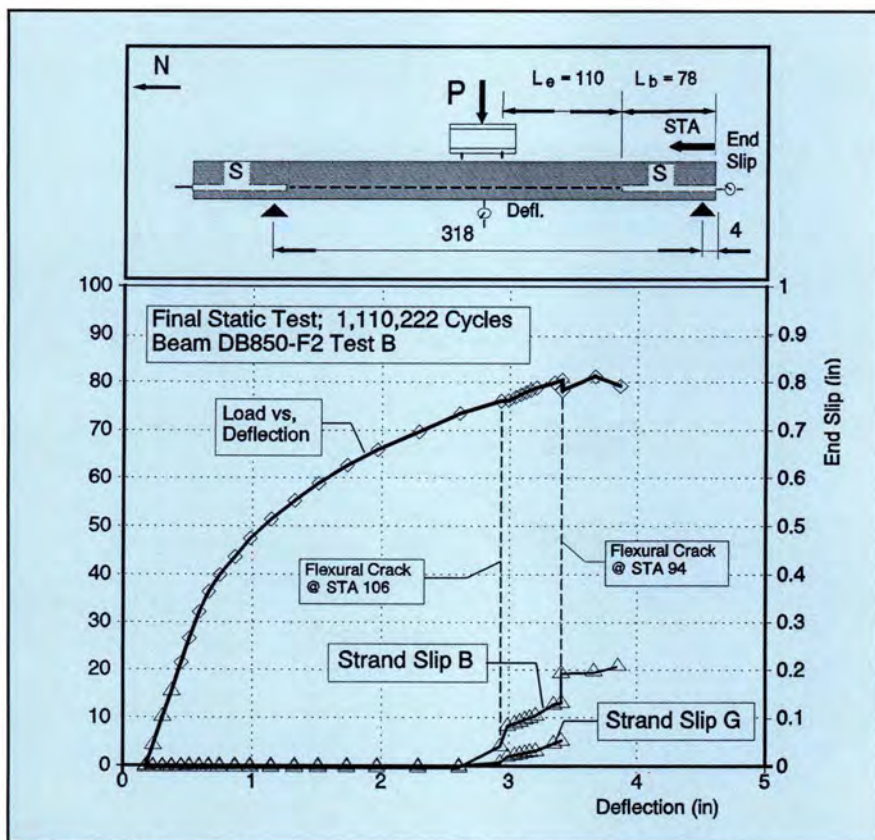


Fig. 14. Load vs. deflection and end slips for Beam DB850-F2, Test B.

beam failed at a load of 82.6 kips (367 kN). The applied moment at failure was 5670 kip-in. (641 kN-m), approximately 94 percent of the calculated flexural capacity. Bond slips at failure were relatively large and, overall, the beam failure must be considered a bond failure. However, the beam behavior was surprisingly similar to a flexural failure, indicated by measurable ductility with final failure brought about by concrete crushing at an average strain of 2470 microstrains.

Beam DB850-F2, Test A

Like Test B on Beam DB850-F1, this test also set an embedment length of 80 in. (2.03 m). However, results from this test were quite different in that significant strand slips resulted directly from repeated applications of service load.

At the initial static test, flexural cracking extended to Station 106, initiating strand slippage that measured approximately 0.09 in. (2.3 mm). The initial static test was followed by fatigue loadings where strand slips increased under the influence of repeated loads. This was the only test in this series where large increases of strand slip occurred as a result of repeated loadings at service load. Strand slips increased from 0.09 in. (2.3 mm) to approximately 0.4 in. (10 mm), resulting only from the action of the repeated load tests.

Results of strand slips and deflections through the different load cycles are summarized in Table 5. Fig. 11 illustrates the loading history and strand slips graphically. The figure depicts the dramatic increase in strand slips as the load cycles increased through the first 26,310 cycles. However, after application of the static load at 26,310 cycles, the increases in strand slips were stabilized.

In the final static test, the beam clearly failed from the loss of bond and strand anchorage. Load vs. deflection and end slip for the final test are shown in Fig. 12. End slips were quite large at the beginning of the test and strand slips increased until failure of the beam. Failure occurred at 63.8 kips (284 kN) and a moment of 4910 kip-in. (555 kN-m), only 82 percent of the calculated ultimate load.

Beam DB850-F2, Test B

The embedment length for this test was set at 110 in. (2.79 m). In earlier static tests reported in Ref. 1, an embedment length of 108 in. (2.74 m) was shown to adequately develop the nominal flexural strength on Beam DB850-3, Test B. The loading history, strand slips and deflections through the cyclic loads are listed in Table 6 and shown graphically in Fig. 13.

The initial static test loaded the beam to $1.3 P_{sv}$, a relatively low initial cracking load to prevent flexural cracking in the debond/transfer zone. The nearest flexural crack to the support formed at Station 142, well outside of the debond/transfer zone. No strand slip was recorded in the initial static test.

During testing, two static overloads were applied to the beam: $1.4 P_{sv}$ at 184,410 cycles and $1.3 P_{sv}$ at 271,194 cycles. No new flexural cracks were formed during application of either load. From examining Table 6, it is seen that the strands did not slip during either the repeated loading or during the intermediate static overloads.

The beam was loaded to failure after 1,110,222 cycles, as shown in Fig. 14. The beam failed at a load of 81.4 kips (362 kN) by crushing of the concrete at the top compression fiber. Strand slips occurred during the final test, coinciding with flexural cracking in the debond/transfer zone. At a load of 76.1 kips (338 kN), a flexural crack formed at Station 106 causing initial strand slips. At 80.9 kips (360 kN), another flexural crack formed at Station 94, causing the strands to slip even more. The beam continued to resist increased loads until failure at 81.4 kips (362 kN), corresponding to a failure moment of 5600 kip-in. (633 kN-m), or 93 percent of the calculated flexural capacity. Concrete strain at crushing was 2416 microstrains.

Beam DB850-F3

Beams DB850-F3 and DB850-F4 differ from the previous two beams in that the debonding pattern for these two beams was "concurrent," meaning that all four of the debonded strands had the same debonded length. The prediction for anchorage failure pre-

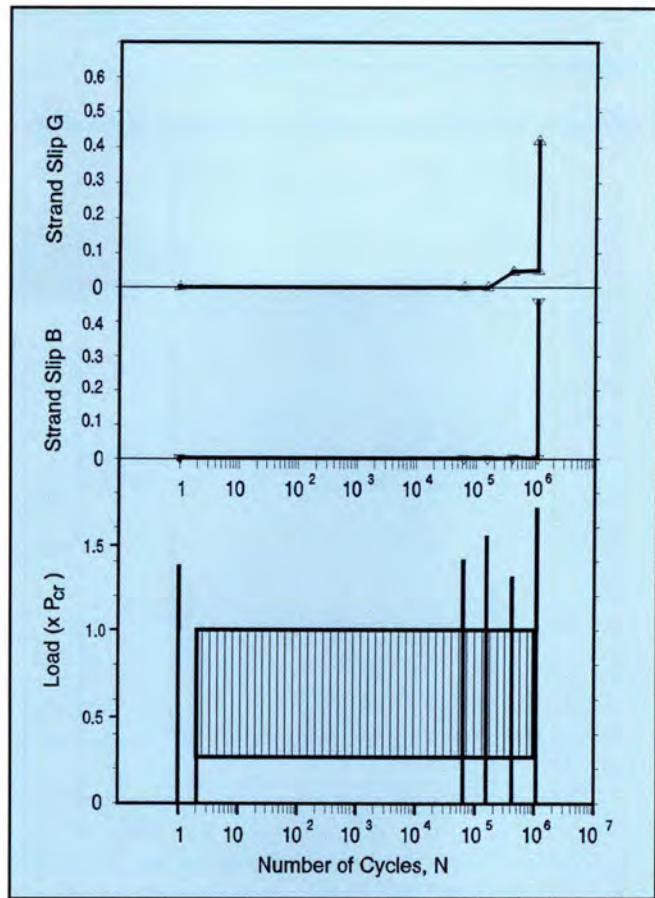


Fig. 15. Strand slips vs. number of load cycles and loading history for Beam DB850-F3.

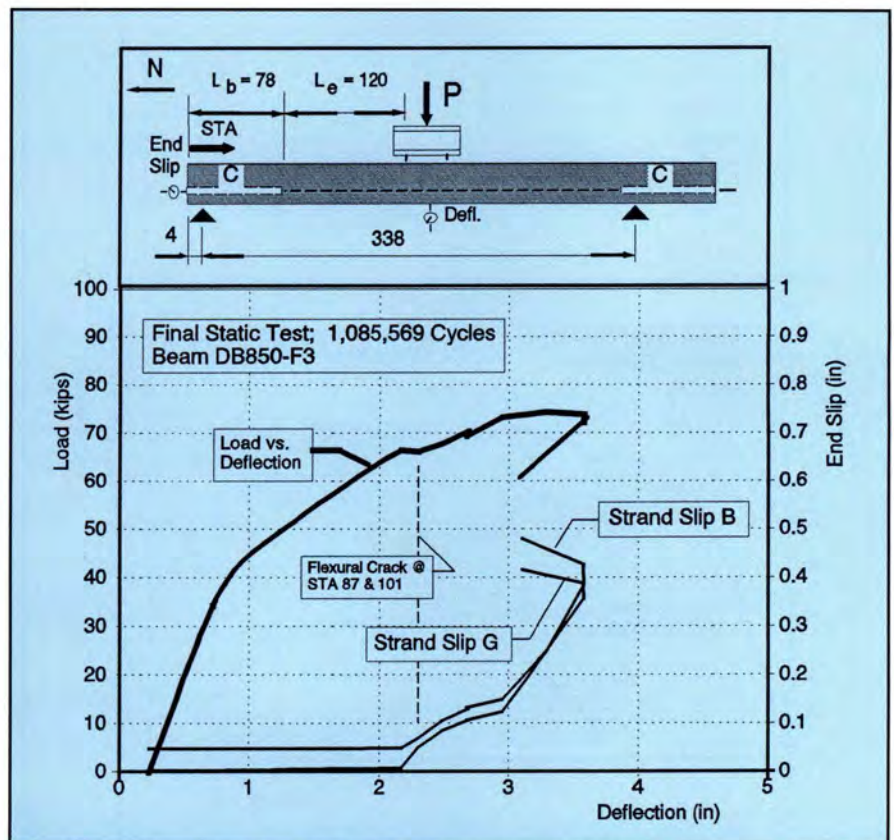


Fig. 16. Load vs. deflection and end slips for Beam DB850-F3.

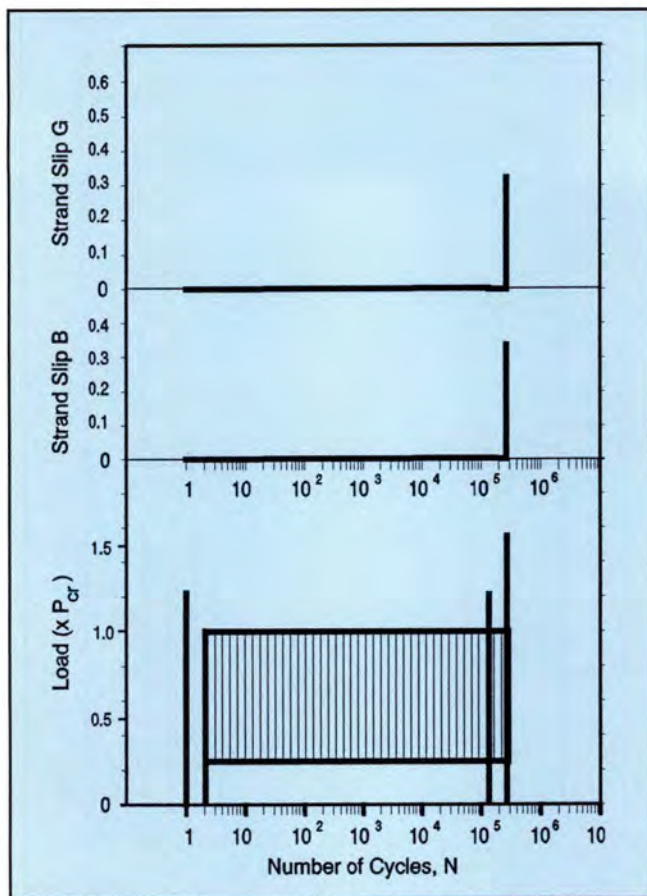


Fig. 17. Strand slips vs. number of load cycles and loading history for Beam DB850-F4.

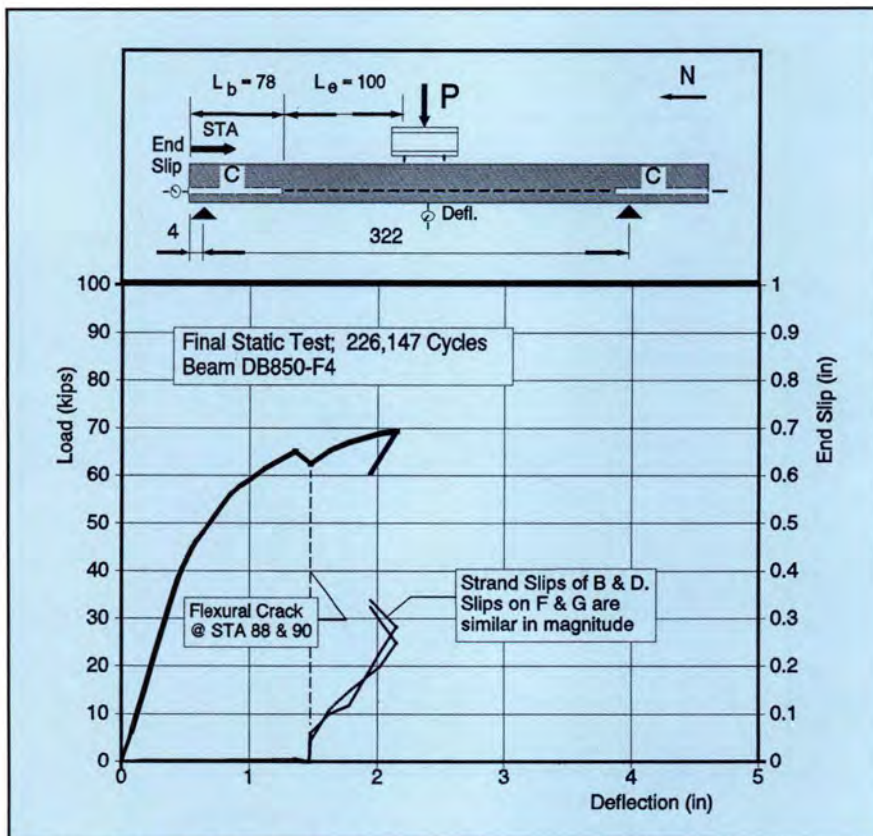


Fig. 18. Load vs. deflection and end slips for Beam DB850-F4.

sented in Ref. 1 showed that longer embedment lengths are required to develop strand anchorages for concurrent debonding patterns.

The embedment length for Beam DB850-F3 was chosen to be 120 in. (3.05 m). In the companion beam, Beam DB850-5A, an embedment length of 120 in. (3.05 m) with concurrent debonding caused bond failure.¹ The loading history for this beam is illustrated in Fig. 15. Values for load magnitude, strand slips and deflection are presented in Table 7.

The initial static load of $1.3 P_{sv}$ caused little or no damage to the anchorage zone of the debonded strands; flexural cracking was limited to 161 in. (4.09 m) from the end of the beam. Repeated loading of 152,000 cycles produced no significant strand slips. At 152,538 cycles, the specimen was loaded to $1.5 P_{sv}$, increasing the load over the previous overloads. Consequently, new flexural cracks formed at Stations 140 and 150; however, measured strand slips from this loading were less than 0.01 in. (0.3 mm).

In subsequent repeated loading between cycles 152,538 and 414,844, the slip on Strand G increased from 0.0002 to 0.0455 in. (0.005 to 1.2 mm). However, these slips are relatively small; and perhaps more importantly, the strand anchorages stabilized and strand slip did not increase in repeated loadings between 414,844 and 1,085,569 cycles.

After 1,085,569 cycles, the beam was tested statically until failure. Load vs. deflection and end slips are shown in Fig. 16. At a load of 67.8 kips (302 kN), flexural cracks formed at Stations 87 and 101. Upon formation of these cracks, strand slips increased dramatically. Additional loading brought about further strand slips until the beam finally failed at a load of 74.2 kips (330 kN), approximately 92 percent of the calculated flexural capacity.

At beam failure, strand slips were measured to be 0.46 in. (11.7 mm) on Strand B and 0.42 in. (10.7 mm) on Strand G. It is interesting to note that the beam did fail in flexure due to the ductility available from the fully bonded strands. However, the evi-

Table 9. Summary of end slips and comparison of cracking in the debond/transfer zone of pretensioned beam specimens.

| Beam | Load cycle, N | Extreme crack; debond/transfer zone | | End slips | | Beam mode of failure |
|-----------|---------------|-------------------------------------|----------|---------------|-----------------------|----------------------|
| | | Maximum load at test (kips) | Station* | Initial slip† | Slip at failure (in.) | |
| DB850-F1A | 1 | 62.3 | 105 | 0.02 | — | Flexure |
| | 1,040,050 | 70.1 | — | — | 0.240 | |
| DB850-F1B | 1 | 58.5 | 130 | 0 | — | Bond |
| | 386,878 | 72.5 | 88 | 0.13 | — | |
| | 1,027,083 | 82.6 | 76 | — | 0.605 | |
| DB850-F2A | 1 | 55.0 | 106 | 0.09 | — | Bond |
| | 192,945 | 63.8 | — | — | 0.676 | |
| DB850-F2B | 1 | 61.6 | 142 | 0 | — | Flexure |
| | 1,110,222 | 81.4 | 94 | 0.20 | 0.20 | |
| DB850-F3 | 1 | 57.7 | 161 | 0 | — | Bond |
| | 152,538 | 65.0 | 140 | 0 | — | |
| | 1,110,222 | 74.2 | 87 | 0.459 | 0.459 | |
| DB850-F4 | 1 | 55.9 | 159 | 0 | — | Bond |
| | 266,147 | 69.3 | 88 | 0.336 | 0.336 | |

Note: 1 kip = 4.448 kN; 1 in. = 25.4 mm.

* Distance from the end of the beam.

† Measured slip at conclusion of static test.

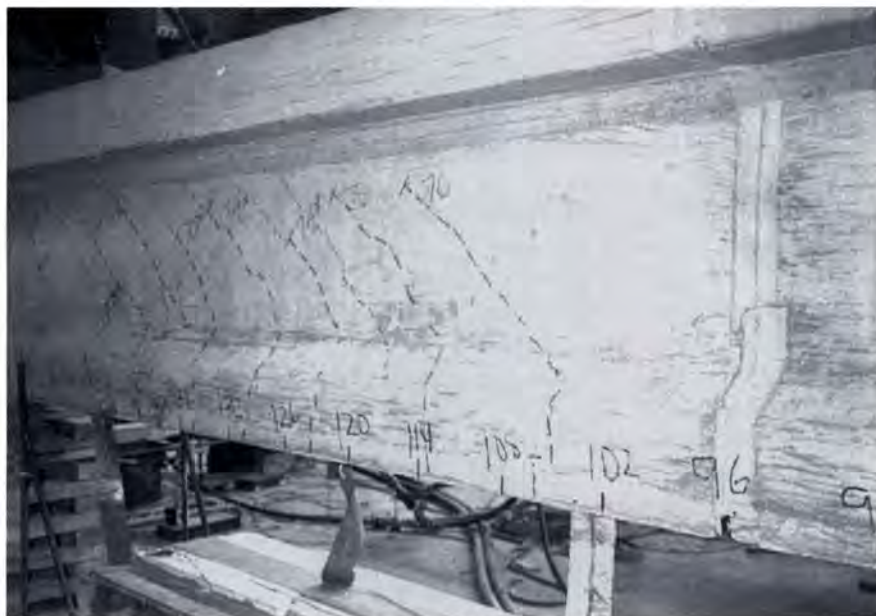


Fig. 19. Test DB850-F2B at load equal to 76 kips (338 kN).

dence of significant strand slips combined with a failure load less than the nominal flexural capacity suggests that failure resulted from a loss of strand anchorage (bond failure).

Beam DB850-F4

The embedment length for this test was set at 100 in. (2.54 m), a relatively short embedment length, to correlate anchorage failure with cracking in the transfer zone. The initial static

loads and the intermediate static loads were relatively small at $1.3 P_{sv}$ to prevent cracking through the anchorage zone through the early portion of testing, and to investigate whether strand slips can occur solely through the action of repeated service loads. The load history and end slips are plotted in Fig. 17 and listed in Table 8. As the figure and table indicate, there were no significant strand slips before the static load to failure.

The static test at 266,147 cycles was

intended to be an intermediate load to $1.6 P_{sv}$; however, the beam failed before this load was achieved. The load vs. deflection and end slips are illustrated in Fig. 18. As noted in the figure, strand slips were initiated by propagation of flexural cracking at Stations 88 and 90 at an applied load of approximately 65 kips (289 kN). Flexural cracks also formed at Stations 102, 103 and 111. Strands D and F, which were also debonded for a length of 78 in. (1.98 m), had strand slips similar in magnitude to Strands B and G.

Beam DB850-F4 failed at an applied load of 69.3 kips (308 kN), approximately $1.5 P_{sv}$ and 87 percent of its calculated flexural capacity. After the initial flexural cracking in the transfer zone of debonded strands, strand slips increased with increasing load and the beam failed in flexure due to a loss of anchorage of the debonded strands. Concrete strains were not measured during this test.

DISCUSSION OF TEST RESULTS

Strand Slips and Cracking in the Debond/Transfer Zone

Table 9 summarizes the incidence of strand slips compared to cracking in the transfer zone of debonded strands. The table lists the load cycle and magnitude for each static overload, provided the magnitude of load exceeded that of previous static tests. Then, for each test, the location of the crack nearest the end of the beam (the "extreme" crack) is shown along with the amount of end slip that was measured at the completion of that particular static test [end slips less than 0.001 in. (0.025 mm) are shown as zero]. From these data it can be seen that, without exception, strand slip was initiated by the formation of flexural cracks through or near the debond/transfer zone. These data demonstrate the critical function of cracking in the disruption of strand anchorage.

For example, consider Test B performed on Beam DB850-F2. Table 6 indicates that no end slips occurred until the final static test. During the final static test to failure, a flexural crack formed at Station 106, as shown



Fig. 20. Test DB850-F2B at load equal to 81 kips (360 kN).

in Fig. 19. As indicated by the marking on the beam, the crack formed at an applied load of 76 kips (338 kN). The load of 76 kips (338 kN) exceeded all previous loads, thus causing new flexural cracks to develop nearer to the end regions.

When this crack formed, strand slips were initiated as shown in Fig. 14. As load was increased to 81 kips (360 kN), another flexural crack formed at Station 94. This crack is shown in Fig. 20. Strand slips increased dramatically, initiated by the new crack propagating through the debond/transfer zone at Station 94.

The plot in Fig. 14 illustrates the relationship between cracking and increases in strand slip. While strand slips caused by cracking at Station 106 were modest, the strand slips increased more dramatically when the concrete cracked at Station 94. The evidence from these two photographs compared to the incidence of strand slippage demonstrates very clearly that cracking disrupts the anchorage zone of the strand, and that these flexural cracks initiated strand slips.

In another example — Beam DB850-F1, Test B — a relatively short embedment length of 80 in. (2.03 m) was chosen to determine the bond deterioration that results from repeated loading as compared to bond deterioration initiated by cracking. As shown in Tables 4 and 9, this specimen demon-

strated that significant strand slips did not occur until flexural cracking propagated through the debond/transfer zone and that strand slips caused by fatigue loadings were less significant.

For the first 386,877 cycles, no cracking occurred near the debond/transfer zone. Not coincidentally, in the absence of cracking no significant strand slips were measured. However, upon application of a larger static overload in test cycle 386,878, flexural cracking formed at Station 88 and strand slips were initiated leading to eventual bond failure.

In Beam DB850-F3, relatively small overloads prevented flexural cracking in the debond/transfer zone for over one million cycles. In the absence of cracking, the strands maintained their anchorage and no strand slips were observed. However, in the final static test to failure, flexural cracks formed at Stations 87 and 101, causing appreciable end slip and subsequent bond failure (Fig. 16).

In every case, despite the number and severity of repeated loads and despite variations in the magnitude and frequency of static overloads, bond slips were initiated by flexural cracking that propagated through the debond/transfer zone. Conversely, if cracking did not propagate through the debond/transfer zone, then strand slips did not occur and strand anchorage was ensured.

From these results, it can be concluded that bond distress and eventual bond failure results directly from cracking that propagates through or near the debond/transfer zone. Furthermore, without cracking near the debond/transfer zone, strand anchorage remained undisturbed through over one million cycles of repeated service loads.

Effects of Repeated Loads on Strand Slips

The strand slip data indicate that large strand slips resulted primarily from the flexural cracking that occurred during the intermediate static overloads. Conversely, the fatigue loading had little effect on the overall bond performance and, in most cases, produced only minor increases in strand slip.

For example, in Test A on Beam DB850-F1, the initial static loading caused a strand slip of 0.02 in. (0.5 mm) that coincided with the formation of a flexural crack at Station 106. In the next 1000 cycles of repeated service loads, strand slips on Strands B and G increased an average of only 0.011 in. (0.03 mm). The next static overload, at load cycle 1023, produced additional strand slips of approximately 0.05 to 0.09 in. (1.3 to 2.3 mm). However, subsequent repeated loadings did not cause any additional strand slips. Instead, strand slips stabilized after the second static loading. In all other tests, except one, strand slips were caused exclusively by large static overloads and not by repeated service loads.

Test A on Beam DB850-F2 represents the only case where significant strand slips occurred during repeated loadings. Strand slips were initiated in the first static test when a flexural crack formed 106 in. (2.69 m) from the end of the beam at a load of 55 kips (245 kN) — see Table 9. Initial slips were small; however, strand slips increased as repeated loads were applied to the beam. Fig. 11 illustrates that strand slips increased from 0.09 in. (2.3 mm) to nearly 0.4 in. (10 mm) in the first 26,310 cycles, demonstrating that bond stresses may be susceptible to fatigue distress from repeated loading.

However, in this case the conditions were very specific for the repeated loads to cause additional bond distress during fatigue loading. In this test, the critical crack formed at the extreme edge of the debond/transfer zone (Station 106) and rendered the strand anchorage susceptible to distress from repeated loads. It is important to note that even in this test, strand slips stabilized after the intermediate static overload applied after 26,310 cycles.

Table 10 reports the measured stresses on Strands B and G on Beam DB850-F2A. Strain gauges attached to Strands B and G in regions of maximum moment indicate that as the strands slipped, their effective prestress was reduced approximately 94 ksi (648 MPa), representing 60 percent of the strands' effective prestress. However, the strands were anchored sufficiently to resist static overloads, as evidenced by increasing strand strains with the application of large external loads. Plots of strand stress are available in Ref. 3.

The results from these tests indicate that, although some bond deterioration occurs due to fatigue loading, the effects of repeated service loads on strand anchorage are small. Furthermore, strand slips and subsequent bond failures result primarily from significant overloads and not from additional distress caused by repeated service loads. While additional strand slips can occur from the effects of fatigue loading, in general, strand slips that resulted from fatigue were relatively small and did not affect the overall beam performance. In every case, strand slips stabilized after a finite number of load cycles and bond failure did not occur solely from repeated service loads.

To summarize, these results indicate that bond fatigue is not important to the overall performance of pretensioned prestressed concrete beams. Even in the one case where significant strand slips were experienced through the application of repeated loads, the total amount of strand slip eventually stabilized; despite large strand slips, sufficient anchorage remained available to these strands to develop bond stresses to resist increases in strand tension that result from application of large static overloads.

First Cracking Loads and Moments

The ability to predict bond slips and subsequent bond failure is dependent on the ability to predict cracking in concrete. In Table 11, first cracking is compared to the predicted cracking load. The results demonstrate remarkable accuracy in predicting cracking loads. Beam DB850-F2B cracked at a load only 94 percent of the predicted load; however, this was the largest disagreement between actual and predicted cracking loads. It should be noted that all of the predicted cracking moments were calculated using the actual tested cylinder strength of the concrete.

Determination of Failure Mode

In these tests, as in many previous test series,^{1,2,3} the primary question is whether or not the strands were able to develop the tension required to produce the nominal flexural capacity of the cross section. Strand slip is evidence that the strand anchorage may be inadequate to develop the required tension; strand slips indicate that the strand bond may have failed. On the other hand, both the static test series and tests with fully bonded strands have provided many examples of strands that slipped and yet the test specimen still achieved its ultimate flexural capacity.¹²

These fatigue tests on beams with debonded strands provide even more examples of strands that have slipped and yet the beams still achieved flexural capacity. For instance, Tests DB850-F1A and DB850-F2B experienced strand slips up to 0.24 in. (6.1 mm), yet each beam was able to achieve a ductile flexural failure at a high percentage of the nominal flexural capacity. It is apparent that small amounts of strand slip do not preclude bond stresses from acting to restrain the strand and resist additional strand tension.

In previous tests on fully bonded beams,^{3,12} it had been relatively simple to differentiate between flexural failure and bond failure. If strands were sufficiently anchored, a beam would fail in flexure. Conversely, if the

Table 10. Change in strand stress for Beam DB850-F2, Test A.

| Load cycle | Strand stress (ksi) | | |
|------------|---------------------|---------|-------|
| | Beginning | Maximum | End |
| 1 | 0 | +54.1 | -4.3 |
| 7000 | -92.5 | -59.5 | -92.5 |
| 26,310 | -98.6 | -64.1 | -98.3 |
| 121,308 | -91.2 | -22.0 | -97.6 |
| 192,945 | -96.1 | -85.4 | -96.8 |

Note: 1 ksi = 6.895 MPa.

* Stress measured by strain gauge attached on Strand B at Station 150.

† Stress = 0 at the effective prestress of 152 ksi.

Table 11. First cracking loads and moments of initial static tests on repeated load tests.

| Beam | First cracking | | |
|-----------|-----------------|------------------|-------------------|
| | P_{cr} (kips) | Moment (kip-in.) | Moment M_{cr} * |
| DB850-F1A | 41.02 | 3281 | 0.96 |
| DB850-F1B | 48.58 | 3337 | 0.98 |
| DB850-F2A | 42.50 | 3273 | 0.96 |
| DB850-F2B | 46.93 | 3231 | 0.94 |
| DB850-F3 | 45.77 | 3393 | 0.99 |
| DB850-F4 | 47.30 | 3359 | 0.98 |

Note: 1 kip = 4.448 kN; 1 kip-in. = 0.113 kN-m;
1 psi = 0.006895 MPa; 1 ksi = 6.895 MPa.

* M_{cr} = 3422 kip-in. (f'_c = 7733 psi, f_r = 7.5 $\sqrt{f'_c}$, and f_{se} = 152 ksi).

strand anchorages were insufficient, then the strands failed in bond.

Flexural failures were characterized by two criteria: capacity and ductility. If a beam reached its nominal flexural capacity and was able to sustain that load through significant deformations, then the failure was a flexural failure. Conversely, anchorage failures were characterized by gross displacements of the strands relative to the concrete (end slips) and either a lessened capacity or an inability to sustain load.

In the static test series on debonded beams, the differences became more difficult to distinguish because hybrid failures occurred where the beams failed in flexure but the strands exhibited some slip. These hybrid failures are caused, in part, by the combination of fully bonded and debonded strands. In many cases, where debonded strands may be losing anchorage as a result of cracking in the debond/transfer zone, the fully bonded strands remain capable of developing the tension required to yield the strands. A typical failure in this case could be a ductile

Table 12. Summary of failure mode and applied load at failure for repeated test loads.

| Beam | L_b (in.) | L_e (in.) | Ultimate load | | | Top fiber strain failure (10^3 in./in.) | Mode of failure |
|-----------|-------------|-------------|---------------|------------------------|----------------------------|--|-------------------|
| | | | P_u (kips) | $M_{u,test}$ (kip-in.) | $\frac{M_{u,test}}{M_n^*}$ | | |
| DB850-F1A | 78(S) | 100 | 70.05 | 5602 | 0.93 | 2606 | Flexure with slip |
| DB850-F1B | 78(S) | 80 | 82.57 | 5672 | 0.94 | 2470 | Bond |
| DB850-F2A | 78(S) | 80 | 63.78 | 4911 | 0.82 | 3080 | Bond |
| DB850-F2B | 78(S) | 110 | 81.37 | 5602 | 0.93 | 2416 | Flexure with slip |
| DB850-F3 | 78(C) | 120 | 74.23 | 5503 | 0.92 | 2092 | Bond |
| DB850-F4 | 78(C) | 100 | 69.34 | 5249 | 0.87 | n/a | Bond |

Note: 1 in. = 0.0254 m; 1 kip = 4.448 kN; 1 kip-in. = 0.113 kN-m.

* The calculated nominal flexural strength, $M_n = 6010$ kip-in.

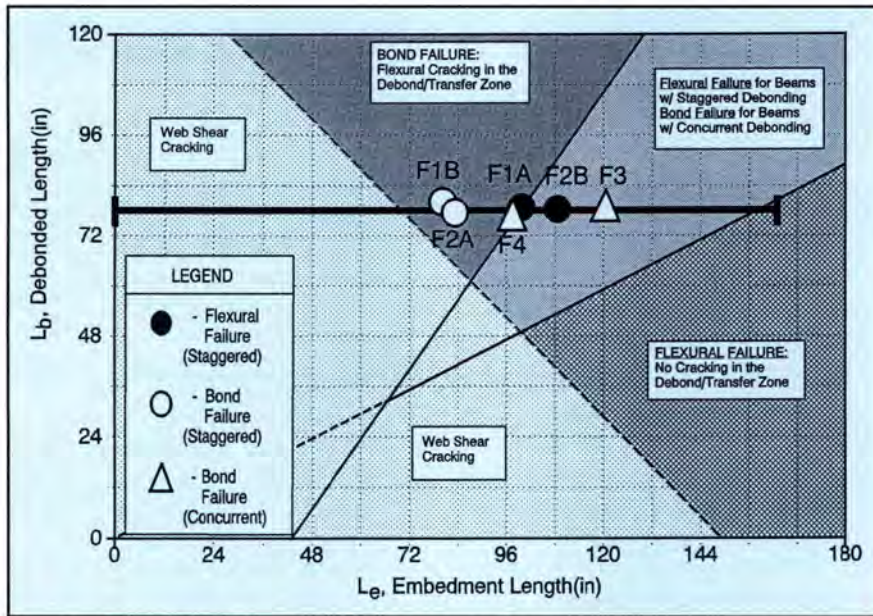


Fig. 21. Comparison of test results to predicted failures.

flexural failure, but the flexural capacity may be reduced.

In these fatigue tests on debonded beams, it is even more difficult to distinguish between flexural failures and anchorage failures. In every test, significant strand slips occurred. However, in some cases, the beams appeared to achieve their flexural capacity. The difficulty is that the apparent flexural failures of Beams DB850-F1A and DB850-F2B occurred at loads that were only about 93 percent of the calculated capacity. In these cases, the concrete crushed in compression at much lower strains than the crushing strains for the static test series.

For example, consider the final static test on Beam DB850-F1A that was performed after 1 million cycles. As shown in Table 3, the beam had 0.29 in. (7.4 mm) of permanent deflec-

tion. Beam DB850-F1A failed when the concrete crushed at a compressive strain of only 0.002480 in./in. Initial concrete strain readings were measured before the first static load was applied, so stated concrete strains include the effects from the total load history of the beam.

If the concrete in Beam DB850-F1A had demonstrated a higher strain capacity, then failure would have occurred at a higher load, similar to its statically tested companion beam. From these data, it is concluded that Beam DB850-F1A failed in flexure even though failure was only 93 percent of the calculated nominal capacity. A similar argument can be made that Beam DB850-F2B also failed in flexure.

Table 12 summarizes the failure mode for each test. Beams DB850-F1A and DB850-F2B failed in flexure.

The embedment lengths for these two tests were 100 and 110 in. (2.54 and 2.76 m), respectively. The other four tests failed in bond with large amounts of bond slips. The applied moments in these tests varied from 82 to 94 percent of the calculated flexural capacity with bond slips that are quite large, on the order of 0.5 in. (13 mm).

Comparison of Results With Predicted Behavior

A behavioral model for the prediction of anchorage failure in beams containing debonded strands was presented in the September-October 1994 issue of the PCI JOURNAL.¹ The premise for the model is that strand anchorage is likely to fail when cracks propagate through the transfer zone of a strand. By predicting the formation of cracks, bond failure is also predicted.

In Fig. 21, the test results from the fatigue test series are overlaid on the prediction model. For beams with staggered debond termination points, the behavioral model predicts flexural failure for embedment lengths in excess of approximately 100 in. (2.54 m) and anchorage failures for embedment lengths less than 100 in. (2.54 m).

Two tests with staggered debonding, Test B on Beam DB850-F1 (F1B) and Test A on Beam DB850-F2 (F2A), clearly failed in bond at embedment lengths of 80 in. (2.03 m). In these tests, flexural cracking that propagated through the transfer zones of debonded strands caused anchorage failure of the pretensioned strands. At failure, strand slips exceeded 0.6 in. (15.2 mm).

Test B on Beam DB850-F1 (F1B) and Test A on DB850-F1 (F2A) both

contained staggered debonding with embedment lengths of 100 and 110 in. (2.54 and 2.79 m), respectively. Results from these two tests are less conclusive, and failures can best be described as hybrid failures that developed ductile failures, but at capacities less than the calculated capacity and with strand slips of approximately 0.2 in. (5 mm). Despite the hybrid failures, the relationship between cracking and bond failure is clearly demonstrated by these two tests. In both cases, cracking in the transfer zones of debonded strands resulted in strand slippage and anchorage failure.

The two tests performed on specimens with concurrent debonding, Beams DB850-F3 and F4, were tested with relatively short embedment lengths, 120 and 100 in. (3.05 and 2.54 m). The behavioral model of Fig. 21 predicts bond failure if the embedment length is less than approximately 156 in. (3.96 m). Both of these tests failed in bond, as expected. Again, the failures from both tests demonstrated that strand slips did not occur until flexural cracking propagated through the transfer zone of the debonded strands; and significantly, strand slips and anchorage failure were not induced by the repetition of service loads to failure.

From these tests, the behavioral model can clearly be used to predict the behavior of pretensioned beams

made with debonded strands. In every case, the formation of cracks through the transfer zones of debonded strands eventually caused bond failure. The two hybrid failures are located close to a "borderline" on the prediction model, so a mixed failure is not entirely unexpected. More significantly, fatigue loading resulted in only slight deterioration of strand anchorage, as evidenced by increasing bond slips.

CONCLUSIONS

1. The behavior of beams made with debonded strands is predictable and reliable. Therefore, the use of debonded strands should be considered safe, provided that the transfer zone of debonded strands is not allowed to extend into regions where cracking will occur at ultimate loading.

2. The formation of flexural cracking through the transfer zones of debonded strands caused the debonded strands to slip. In every case, strand slip was initiated by a crack through the debond/transfer zone.

3. Fatigue loading had a small detrimental effect on strand anchorage. While fatigue loading did cause small increases in strand slip, in every case strand slip stabilized after a finite number of loads or after application of a static load, and subsequent beam failure was governed by beam behavior under static loads.

4. Bond failures in beams with debonded strands resulted in ductile failures, even though the flexural strength of the beam was reduced from its calculated nominal flexural capacity.

RECOMMENDATIONS

1. Debonded strands should be allowed as an alternative to draped strands; however, the debond/transfer zone should not extend into regions of flexural cracking.

2. Debond termination points should be staggered to increase the beam's resistance to cracking in the debond/transfer zone.

ACKNOWLEDGMENT

The research described in this paper was part of a research project sponsored by the U.S. Department of Transportation, Federal Highway Administration, through the Texas Department of Transportation. Their support of the project, "Influence of Debonding of Strands on Behavior of Composite Prestressed Concrete Bridge Girders," is gratefully acknowledged by the authors. The authors also commend Florida Wire and Cable Company for their contribution of prestressing strand.

REFERENCES

1. Russell, Bruce W., Burns, Ned H., and Zumbrennen, Leslie G., "Predicting the Bond Behavior of Prestressed Concrete Beams Containing Debonded Strands," *PCI JOURNAL*, V. 39, No. 5, September-October 1994, pp. 60-77.
2. Zumbrennen, Leslie G., Russell, Bruce W., and Burns, Ned H., "Behavior of Statically Loaded Pretensioned Concrete Beams With 0.5 inch Diameter Debonded Strands," Research Report 1210-4, Center for Transportation Research, The University of Texas at Austin, Austin, TX, January 1992, 110 pp.
3. Russell, Bruce W., and Burns, Ned H., "Design Guidelines for Transfer, Development and Debonding of Large Diameter Seven Wire Strands in Pretensioned Concrete Girders," Research Report 1210-5F, Center for Transportation Research, The University of Texas at Austin, Austin, TX, January 1993, 286 pp.
4. ACI Committee 318, "Building Code Requirements for Reinforced Concrete (ACI 318-89)," American Concrete Institute, Detroit, MI, 1989.
5. AASHTO, *Standard Specifications for Highway Bridges*, 14th Edition, American Association of State Highway Transportation Officials, Inc., Washington, D.C., 1989.
6. Kaar, Paul H., and Magura, Donald D., "Effect of Strand Blanketing on Performance of Pretensioned Girders," *PCI JOURNAL*, V. 10, No. 6, December 1965, pp. 20-34.
7. Rabbat, B. G., Kaar, P. H., Russell, H. G., and Bruce, R. N., Jr., "Fatigue Tests of Pretensioned Girders with Blanketed and Draped Strands," *PCI JOURNAL*, V. 24, No. 4, July-August 1979, pp. 88-114.
8. Dane, John III, and Bruce, R. N., Jr., "Elimination of Draped Strands in Prestressed Concrete Girders," Technical Report No. 107, State of Louisiana, June 1975.
9. Janney, Jack R., "Nature of Bond in Pre-Tensioned Prestressed Concrete," *ACI Journal*, V. 25, No. 5, May 1954, pp. 717-736.
10. Hanson, Norman W., and Kaar, Paul H., "Flexural Bond Tests of Pretensioned Prestressed Beams," *ACI Journal*, V. 30, No. 1, January 1959, pp. 783-802.
11. Russell, Bruce W., and Burns, Ned H., "Static and Fatigue Behavior of Pretensioned Bridge Girders Made With High Strength Concrete," *PCI JOURNAL*, V. 38, No. 3, May-June 1993, pp. 118-128.
12. Lutz, B. A., Russell, B. W., Burns N. H., and Kreger, M., "Measurement of Development Length of 0.5 inch and 0.6 inch Diameter Prestressing Strands in Fully Bonded Concrete Beams," Research Report 1210-3, Center for Transportation Research, The University of Texas at Austin, Austin, TX, February 1992.
13. Overman, T. R., Breen, J. E., and Frank, K. H., "Fatigue Behavior of Pretensioned Concrete Girders," Research Report 320-2F, Center for Transportation Research, The University of Texas at Austin, Austin, TX, November 1984.
14. Kaar, Paul H., and Hanson, Norman W., "Bond Fatigue Tests of Beams Simulating Pretensioned Concrete Cross-ties," *PCI JOURNAL*, V. 20, No. 5, September-October 1975, pp. 65-80.
15. Bachman, P. M., Kreger, M. E., and Breen, J. E., "An Exploratory Investigation of Shear Fatigue Behavior of Prestressed Concrete Girders," Research Report 465-1, Center for Transportation Research, The University of Texas at Austin, Austin, TX, June 1987.
16. Zia, P., Preston, H. K., Scott, N. L., and Workman, E. B., "Estimating Prestress Losses," *Concrete International*, V. 1, No. 6, June 1979, pp. 32-38.
17. *PCI Design Handbook*, Fourth Edition, Precast/Prestressed Concrete Institute, Chicago, IL, 1992.
18. Unay, I. O., Russell, B. W., and Burns, N. H., "Measurement of Transfer Length on Prestressing Strands in Prestressed Concrete Specimens," Research Report 1210-1, Center for Transportation Research, The University of Texas at Austin, Austin, TX, March 1991, 135 pp.